

## Prediction of Indian Summer Monsoon Onset Using Dynamical Subseasonal Forecasts: Effects of Realistic Initialization of the Atmosphere

ANDREA ALESSANDRI,<sup>\*</sup> ANDREA BORRELLI,<sup>+</sup> ANNALISA CHERCHI,<sup>#</sup> STEFANO MATERIA,<sup>+</sup>  
ANTONIO NAVARRA,<sup>#</sup> JUNE-YI LEE,<sup>@</sup> AND BIN WANG<sup>&</sup>

<sup>\*</sup> Agenzia Nazionale per le nuove Tecnologie, l'energia e lo sviluppo economico sostenibile,  
Rome, Italy, and International Pacific Research Center, Honolulu, Hawaii

<sup>+</sup> Centro Euro-Mediterraneo sui Cambiamenti Climatici, Bologna, Italy

<sup>#</sup> Centro Euro-Mediterraneo sui Cambiamenti Climatici, and Istituto Nazionale di Geofisica e Vulcanologia, Bologna, Italy

<sup>@</sup> Research Center for Climate Sciences, Pusan National University, Busan, South Korea

<sup>&</sup> International Pacific Research Center, Honolulu, Hawaii

(Manuscript received 6 June 2014, in final form 26 September 2014)

### ABSTRACT

Ensembles of retrospective 2-month dynamical forecasts initiated on 1 May are used to predict the onset of the Indian summer monsoon (ISM) for the period 1989–2005. The subseasonal predictions (SSPs) are based on a coupled general circulation model and recently they have been upgraded by the realistic initialization of the atmosphere with initial conditions taken from reanalysis. Two objective large-scale methods based on dynamical-circulation and hydrological indices are applied to detect the ISM onset. The SSPs show some skill in forecasting earlier-than-normal ISM onsets, while they have difficulty in predicting late onsets. It is shown that significant contribution to the skill in forecasting early ISM onsets comes from the newly developed initialization of the atmosphere from reanalysis. On one hand, atmospheric initialization produces a better representation of the atmospheric mean state in the initial conditions, leading to a systematically improved monsoon onset sequence. On the other hand, the initialization of the atmosphere allows some skill in forecasting the northward-propagating intraseasonal wind and precipitation anomalies over the tropical Indian Ocean. The northward-propagating intraseasonal modes trigger the monsoon in some early-onset years. The realistic phase initialization of these modes improves the forecasts of the associated earlier-than-normal monsoon onsets. The prediction of late onsets is not noticeably improved by the initialization of the atmosphere. It is suggested that late onsets of the monsoon are too far away from the start date of the forecasts to conserve enough memory of the intraseasonal oscillation (ISO) anomalies and of the improved representation of the mean state in the initial conditions.

### 1. Introduction

The Indian summer monsoon (ISM) rainfall concentrated between June and September represents more than 70% of the annual precipitation over the Indian subcontinent (Parthasarathy et al. 1994). Its rapid onset at the southern tip of India (Kerala) is followed by a northward progression of the rainfall with the establishment of the monsoon at northern locations (Webster et al. 1998; Goswami 2005). The monsoon onset is an important event for agricultural planning, food production,

and the lives of over one billion people (Wang et al. 2009; Goswami et al. 2010). Because human and agricultural activities strongly depend on the onset of the rainy season and its northward progression, which are highly variable from year to year (i.e., Webster et al. 1998), prediction of the monsoon onset is of paramount importance for India and its inhabitants. Back in 1943, the India Meteorological Department (IMD) prepared diagrams with isopleths of the normal dates of the monsoon onset over India based on rainfall data at a large number of stations (India Meteorological Department 1943). Based on these diagrams, operational forecasters at IMD have determined the date of monsoon onset every year over Kerala using daily rainfall reports from rain gauge stations of the synoptic network. For many years, the criteria for the detection of the monsoon onset did not consider specific quantitative thresholds, hence, the

---

Corresponding author address: Andrea Alessandri, Agenzia Nazionale per le nuove Tecnologie, l'energia e lo sviluppo economico sostenibile, Via Anguillarese, 301 Sp. 118 CR Casaccia, 00123 Santa Maria di Galeria, Rome, Italy.  
E-mail: andrea.alessandri@enea.it

estimates were considered subjective (Joseph et al. 2006). Recently, IMD adopted an objective identification of the monsoon onset by combining estimates of precipitation, winds, and OLR and identifying specific thresholds and temporal evolution based on observations (Joseph et al. 2006). In fact, during the monsoon onset over India, the rapid increase in daily precipitation rate is accompanied by other dramatic changes, like an increase in the vertically integrated moisture of the atmosphere, the wind, and the kinetic energy, especially at lower levels (Krishnamurti 1985). Therefore, low-level winds and tropospheric moisture buildup over south of the Indian peninsula have been widely used as indicators of monsoon onset (i.e., Pearce and Mohanty 1984; Ju and Slingo 1995; Cherchi and Navarra 2003; Taniguchi and Koike 2006). Based on the principal component regression technique of large-scale circulation features and rainfall over Kerala, Pai and Nair (2009) describe the empirical tool, in use at IMD starting from 2005, for the prediction of the ISM onset over Kerala one month in advance. Even though the tool is not suited to provide probabilistic consideration of the predictions, the authors report some deterministic skill for the retrospective forecasts covering the period from 1997 to 2007 with an RMSE of about 4 days, which is much less compared to RMSE of the predictions from a climatology-based model (7.32 days) during the same period.

Traditionally, the onset of the monsoon is primarily defined by precipitation because it is the parameter that mostly affects living activities. However, the prediction of monsoon onset dates based on precipitation from the rain gauge stations of the synoptic network has many disadvantages. First, precipitation is a difficult field to monitor and its prediction is especially problematic because of the complexity of spatial and temporal gradients involved (Fasullo and Webster 2003). Second, even though the last generation of state-of-the-art coupled general circulation models (CGCMs) achieved some improvement, the observed monsoon mean rainfall pattern and variability are still poorly modeled (Sperber et al. 2013). On the other hand, atmospheric wind and moisture are generally well represented by models (Fasullo and Webster 2003; Lee et al. 2011) and are, therefore, suitable for forecasting studies, as soon as they can be easily used for objective identification of the monsoon onset (Wang et al. 2009). Moreover, atmospheric fields over a single district (like Kerala) could hardly diagnose the planetary-scale monsoon (Soman and Kumar 1993; Joseph et al. 1994) while being susceptible to “bogus” (false) monsoon onsets mostly connected with disturbances not related to the monsoon (Flatau et al. 2001; Stephens et al. 2004). Often bogus onsets are followed by extended periods of weak winds

and clear skies associated with droughts over India that could cause disastrous economic and agricultural damages (i.e., crops failure because of lack of water after plantation) if not correctly predicted (Fasullo and Webster 2003; Webster 2013), as it happened in 2002 (Webster and Hoyos 2004). Examples of large-scale and objective indicators of Indian monsoon onset dates suitable for the verification of numerical model performance and their forecasts are given by Fasullo and Webster (2003) and by Wang et al. (2009). In particular, Fasullo and Webster (2003) introduced a hydrological definition of the monsoon onset and withdrawal using the vertically integrated moisture transport. Wang et al. (2009) determined the monsoon onset by the beginning of the sustained 850-hPa zonal wind averaged over the southern Arabian Sea. Both indices are based on fields that are better modeled and measured than rainfall, and they are both linked with the large-scale monsoon circulation.

The dynamical subseasonal to seasonal prediction of the Indian monsoon rainfall is still a challenge (Krishnamurthy and Shukla 2011), as dynamical models have significant problems in the representation of the mean Indian monsoon climate and its variations on different time scales (i.e., Gadgil and Sajani 1998; Kang et al. 2002; Wang et al. 2004, 2005; Rajeevan and Nanjundiah 2009; Sperber et al. 2013). Results of works attempting to forecast monsoon interannual variability with dynamical models indicate skill limitations due to (i) biases, (ii) processes misrepresentation, and (iii) initialization errors of the coupled models (Lee et al. 2010; Krishnamurthy and Shukla 2011; Rajeevan et al. 2012). For example in the DEMETER (Palmer et al. 2004) coupled models ensemble, the skill of seasonal forecasts of the monsoon is positive, though generally modest, and it is larger for the earlier period of the hindcasts (i.e., 1959–79) rather than for the more recent period (1980–2001; Preethi et al. 2010). Later multimodels exercises of seasonal forecasts, such as ENSEMBLES (Weisheimer et al. 2009; Alessandri et al. 2011), were recognized having a better skill, for example, in the prediction of monsoon droughts (Rajeevan et al. 2012). However, despite some predictability of the interannual anomalies of seasonal mean ISM strength (Gadgil and Sajani 1998; Kang et al. 2002; Preethi et al. 2010; Krishnamurthy and Shukla 2011; Rajeevan et al. 2012, among others), the skill in predicting the onset of the monsoon is still very poor (e.g., Cherchi and Navarra 2003; Li and Zhang 2009). The northward-propagating onset phase and the subsequent active and break spells of the monsoon are often associated with the summer intraseasonal oscillations (ISOs; Krishnamurti 1985; Webster et al. 1998; Lee et al. 2013; Seo et al. 2007). In particular, the analysis of the observational dataset collected during 1979 for the

Summer Monsoon Experiment (MONEX; Krishnamurti 1985), showed that the onset and the active/break phases of the monsoon can be related to the passage of northward-propagating ISO systems. During the MONEX experiment a sequence of ISO wind anomalies at 850 hPa in the 30–50-day frequency band have been shown to meridionally propagate troughs and ridges from near equator, then amplify as they arrive close to the Indian subcontinent at 10°N, and finally dissipate as they arrive near Himalayas foothills (Krishnamurti and Subrahmanyam 1982). As discussed in Krishnamurti and Subrahmanyam (1982), the broadscale monsoon circulation is strengthened by the passage of the trough lines over the Indian subcontinent. During the developing phase of the monsoon in May, the passage of ISO troughs may, therefore, trigger earlier-than-normal monsoon onset. Previous works showed some skill of the prediction systems based on CGCMs in forecasting the boreal summer ISOs over the northern Indian Ocean and Southeast Asia. In the DEMETER coupled models ensemble, realistic northeastward propagation of the ISOs was evidenced over the Indian Ocean during boreal summer and the well-organized observed modes in May–June are almost reproducible from one year to another, whereas in the models these patterns are much more variable (Xavier et al. 2007). Fu et al. (2009, 2011) showed that, by suitably initializing the atmosphere, useful ISO prediction skills can be achieved over Southeast Asia for lead times of 2–3 weeks. These results are confirmed in the framework of the ongoing multimodel Intraseasonal Variability Hindcast Experiment (ISVHE; Lee et al. 2015; Neena et al. 2014), with results showing the skill of some models reaching 3–4 weeks for boreal summer ISOs (Lee et al. 2015). Fu et al. (2009, 2011, 2013) showed that realistic initialization of intraseasonal oscillations can lead to some skill in forecasting monsoon active and break phases at the intraseasonal time scale, with some skill reaching 20–25 days. Still unanswered, however, is whether realistic ISO initialization can improve predictability of ISM onset.

In this work we apply two objective large-scale indices, based (i) on dynamical circulation as defined by Wang et al. (2009) and (ii) on hydrological property as in Fasullo and Webster (2003), to detect the ISM onset in the subseasonal forecasts performed using the prediction system developed at Centro Euro-Mediterraneo sui Cambiamenti Climatici (CMCC). We evaluate the performance of the retrospective subseasonal forecasts initialized on 1 May to predict interannual onset anomalies, including the probabilistic skill in capturing earlier or later-than-normal onset dates. The effect on the forecasts of the recent development of the prediction system

to include a realistic initialization of the atmospheric component from reanalysis data is assessed in detail. The present study is organized as follows: section 2 defines the methodology by describing the prediction system considered, the observations/reanalysis dataset used for verification and the procedure for the detection of the ISM onset. Section 3 reports the performance in simulating the intraseasonal variability (section 3a) and in predicting the ISM onset (section 3b). In section 4, the sensitivity of the forecasts of early and late monsoon onsets to the realistic initialization of the atmospheric model component is evaluated by comparison with control hindcasts with not properly initialized atmosphere (i.e., atmosphere simply initialized from AMIP-type historical simulations). Finally, in section 5 a discussion and a summary of the main results are given.

## 2. Method

### a. Prediction system

In the present study, we use the CMCC prediction system (Alessandri et al. 2010, 2011; Borrelli et al. 2012; Matera et al. 2014), as developed for the subseasonal time scale in the framework of the multimodel ISVHE (Lee et al. 2015; Neena et al. 2014).

#### 1) MODEL COMPONENTS

The CGCM included in the CMCC Subseasonal Prediction System (CMCC-SSPS) is the physical core (i.e., with the carbon cycle dynamics turned off) of the CMCC Earth System model (Fogli et al. 2009; Vichi et al. 2011; Alessandri et al. 2012). The coupled model has ECHAM5.3, SILVA, OPA8.2, and LIM as atmospheric, land surface, oceanic and sea ice components. ECHAM5.3 (Roeckner et al. 1996, 2003, 2006) is a global spectral model and the version used here is truncated at the zonal wavenumber 63 with 19 vertical sigma levels. The associated Gaussian grid in which the physical fields are calculated corresponds to a horizontal resolution of about 200 km. The land surface–vegetation model SILVA (Alessandri 2006; Alessandri et al. 2007, 2012) is coupled with the atmospheric component by means of an implicit numerical scheme and von Neumann closure at the surface (Alessandri et al. 2007). OPA8.2 (Madec et al. 1998) is configured on an irregular ORCA2 grid with the horizontal resolution variable in space (it has a nominal resolution of 1.5° in latitude and 2° in longitude, with an increase to 0.5° latitude near the equator) and 31 vertical levels with 10-m resolution in the top 100 m. OPA8.2 is coupled to the sea ice module LIM (Timmermann et al. 2005) with the same horizontal

resolution. The fluxes between the atmosphere and the ocean are exchanged daily (Scoccimarro et al. 2007; Fogli et al. 2009) through the coupler OASIS3 (Valcke et al. 2000) without flux adjustment.

## 2) INITIALIZATION STRATEGY

The initial conditions for the ocean–atmosphere system are prepared offline and independently for the atmosphere and for the ocean. The ocean initialization uses data assimilation products made available by CMCC-INGV Global Ocean Data Assimilation (CIGODAS; DiPietro and Masina 2009; Bellucci et al. 2007; Masina et al. 2011). CIGODAS is based on the assimilation of temperature and salinity profiles using an optimal interpolation assimilation scheme and it is forced with flux data from the 40-yr European Centre for Medium-Range Weather Forecasts (ECMWF) Re-Analysis (ERA-40; Uppala et al. 2005) before 2002 (ERA-40 only covers up to August 2002) and from the ECMWF operational analysis (Andersson and Thépaut 2008) after 2002.

The atmospheric component is initialized with data from the ERA-Interim (Berrisford et al. 2009; Dee et al. 2011). In the CMCC-SSPS, atmospheric 3D prognostic variables (i.e., temperature, specific humidity, divergence, and vorticity) are interpolated from the 60 hybrid levels of ERA-Interim to the 19 hybrid levels of ECHAM5 through Interpolation of ECMWF Re-Analysis data (INTERA; Kirchner 2001). Subsequently, in order to fit into the model, the atmospheric initial state have been horizontally interpolated from the ERA-Interim resolution (T255, corresponding to an associated Gaussian grid of approximately  $79\text{ km} \times 79\text{ km}$ ) to ECHAM5 resolution (T63, corresponding to Gaussian grid of approximately  $1.9^\circ \times 1.9^\circ$ ) [for details see Borrelli et al. (2012)]. The surface temperature at the interface with the atmosphere, the soil moisture, and the snow depth are started with the corresponding ERA-Interim fields in order to avoid a coupling shock at the beginning of the hindcasts. For the soil moisture, we use the wetness of the four soil water layers included in TESSEL (i.e., the land surface model used in the ECMWF reanalysis system; Dee et al. 2011) to estimate the water content into the two soil reservoirs implemented in SILVA. The water content, relative to saturation condition, in the upper (lower) soil layers of SILVA are simply computed as the weighted average of the soil wetness of layers 1 and 2 (3 and 4) of TESSEL. In the CMCC-SSPS, the uncertainty that characterizes the initial state of the system is accounted for by using an ensemble of perturbed atmospheric initial conditions (ICs) [i.e., taking slightly lagged initial states from the atmospheric reanalysis; see section 2a(3) for details].

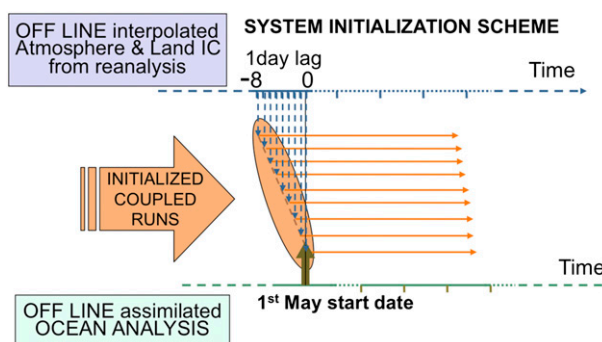


FIG.1. Scheme summarizing the hindcasts production strategy adopted. For each start date, oceanic ICs are obtained from offline forced ocean analysis. For the atmospheric component, an ensemble of nine atmospheric initial states is produced by taking lagged ICs for each start date (i.e., the atmospheric IC are sampled by taking the actual start date and also the 8 days before sampled every 24 h). See section 2a(3) for further details.

## 3) SETUP OF THE EXPERIMENTS

The system described in section 2a(1) is employed to perform a set of retrospective forecasts covering 17 years (1989–2005; hereafter the ERAINI experiment). Every year, the model is initialized on the first of May (Fig. 1) and then integrated for 2 months. To account for the uncertainties that characterize the initial state of the system, an ensemble of nine perturbed atmospheric ICs is prepared for each start date by taking lagged states from the days preceding 1 May (Fig. 1). Other than the actual 1 May IC, the eight preceding states from ERA-Interim are sampled daily and imposed as perturbed atmospheric ICs (Fig. 1). In this way, we obtain nine different initial states from which the SSPs evolve producing a probability distribution of the forecast.

To assess the effect of realistic atmosphere initialization, a control set of predictions (hereafter AMIPINI experiment) is performed taking the same ICs for all the coupled model components but the atmosphere, for which we do not use reanalysis to constrain the atmospheric ICs to the actual initial state. In contrast, the atmosphere ICs for AMIPINI are taken from one of the infinite deterministic trajectories sampled by an AMIP-type simulation performed using the atmospheric model forced with the observed sea surface temperature (SST) from the Met Office Hadley Centre Global Sea Ice and SST dataset (HadISST1.1; Rayner et al. 2003). The AMIPINI experiment use the same perturbation strategy as in ERAINI so that the atmosphere IC from 1 May as well as from the eight preceding days of the AMIP-type simulation are taken to obtain an ensemble of nine atmospheric ICs for each start date of the hindcasts.

### b. Observations/reanalysis

For the verification of the forecasts, we use atmospheric wind and specific humidity from the ERA-Interim (Berrisford et al. 2009; Dee et al. 2011) and NOAA interpolated outgoing longwave radiation (OLR; Liebmann and Smith 1996). Verification data are interpolated at the same T63 horizontal grid of the atmospheric model. Both model and observation/reanalysis anomalies are defined as deviations from the respective climatology for the period 1989–2005.

The ISM onset dates issued by IMD using the criteria adopted in 2006, based on rainfall, wind field, and OLR (Joseph et al. 2006) are also used to compare the results of ISM onset obtained using the objective large-scale indices.

### c. Detection of the ISM onset

To be conveniently applied to forecasts based on CGCMs outputs, the indices for the detection of the ISM onset must be objective, use variables that are well represented by models such as atmospheric wind and moisture (Fasullo and Webster 2003; Lee et al. 2011), and consider sufficiently large-scale domains in order to avoid susceptibility to bogus events. Following this guideline, in this work we choose two indices based (i) on the dynamical circulation (Wang et al. 2009) and (ii) on the hydrological property (Fasullo and Webster 2003), as described in the following subsections.

#### 1) THE ONSET CIRCULATION INDEX

As discussed in Wang et al. (2009) the onset circulation index (OCI) is defined as the 850-hPa zonal wind averaged over the south Arabian Sea area ( $5^{\circ}$ – $15^{\circ}$ N,  $40^{\circ}$ – $80^{\circ}$ E) and it provides a very good estimate of the ISM onset dates. As reported in Wang et al. (2009), the correlation coefficient between the subjective onset dates issued by the IMD for the period 1948–2007 and the respective onset date obtained applying the OCI index to NCEP–NCAR atmospheric reanalysis is 0.81. Following Wang et al. (2009), we detect the onset of the monsoon as the time at which the index exceeds specific thresholds for at least 7 consecutive days. In the reanalysis, the threshold has been chosen to have the climatological OCI onset corresponding with the averaged IMD onset during 1989–2005 (i.e., 3 June). In the forecasts, the threshold has been corrected in order to account for the bias in the modeled OCI, which tends to be larger than in the reanalysis. To this aim, the onset threshold of the forecasts has been increased by the difference in the OCI climatology between predictions and ERA-Interim at the plateau phase that is reached

after the monsoon is well established (period between 10 and 30 June; not shown).

To check the robustness of the results, we computed the ISM onset dates using also 5 and 3 days as the minimum above-threshold consecutive time required to declare onset. We found no appreciable difference of the prediction performance with respect to reanalysis by changing this time length. The only difference is that by decreasing the required time to 5 and 3 days, there is a tendency to reduce the correlation with IMD of the onset dates computed with both reanalysis and forecasts, due to a reduced ability of the detection method to discern bogus events.

#### 2) THE HYDROLOGIC ONSET AND WITHDRAWAL INDEX

According to Fasullo and Webster (2003), the Hydrologic Onset and Withdrawal Index (HOWI) is defined by the vertically integrated moisture transport (VIMT) averaged over the grid points of the domain ( $20^{\circ}$ S– $30^{\circ}$ N,  $40^{\circ}$ – $100^{\circ}$ E) with the more rapid transition of the VIMT from the week before and the week after the climatological monsoon onset. By considering an averaging scale of the VIMT of  $\sim 2 \times 10^6 \text{ km}^2$ , we selected the 50 grid points of the domain with the largest VIMT magnitude change. This was performed independently for the forecasts and for reanalysis, after interpolation of the reanalysis to the same horizontal resolution of the forecasts data ( $\sim 1.9^{\circ} \times 1.9^{\circ}$  longitude–latitude). To check the robustness of the results to the averaging scale, we assessed the effect of halving ( $\sim 1 \times 10^6 \text{ km}^2$ ) and doubling ( $\sim 4 \times 10^6 \text{ km}^2$ ) the averaging domain finding no appreciable difference of the results. Following Fasullo and Webster (2003), the averaged-VIMT time series ( $\chi$ ) is normalized by the transformation:

$$\chi_n = 2 \times \{[\chi - \min(\bar{X})]/[\max(\bar{X}) - \min(\bar{X})]\} - 1, \quad (1)$$

where  $\bar{X}$  is the climatological seasonal cycle and  $\chi_n$  is the normalized time series, such that the climatological seasonal cycle ranges from  $-1$  to  $1$ . The monsoon onset is defined by the times of year at which the ( $\chi_n$ ) index exceeds zero for at least 7 consecutive days.

#### 3) ISM ONSET DATES IN THE REANALYSIS

As the reference for the forecasts, we identify beforehand the ISM onset dates for the period from 1989 to 2005 in the reanalysis using OCI and HOWI and compare the results obtained between the two indices. For completeness, the ISM onset dates issued by IMD (Joseph et al. 2006) are also reported. The ISM onset dates identified by the HOWI, OCI, and those issued by IMD are shown in Fig. 2 in standard deviation units. OCI and HOWI are in good agreement between each

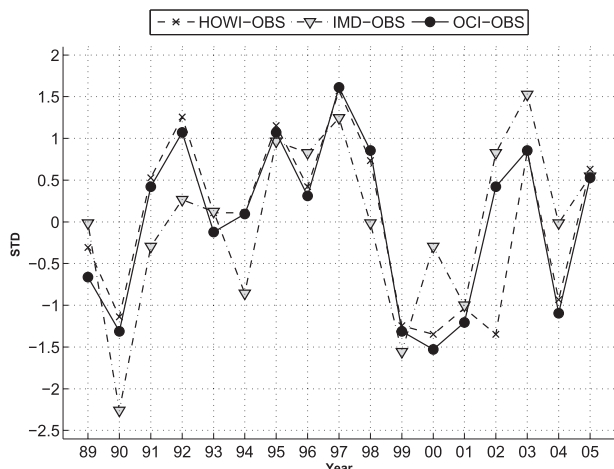


FIG. 2. Normalized anomalous onset dates of the monsoon as diagnosed by OCI (solid line with filled circles) and HOWI (dashed line with  $\times$  marks) indices applied to the ERA-Interim. The dot-dashed line (triangle marks) refers to the onset date definition by IMD.

other (the correlation coefficient is 0.91); they only differ significantly in 2002 when they have opposite values. Using HOWI, 2002 has an early onset date, while using OCI it has a slightly late onset date, in better accordance also with the results from the IMD. As discussed in Joseph et al. (2006), feeble convection and moisture growth were generated in 2002 by premonsoon thunderstorm activity from early to mid-May over the southeast Arabian Sea (Flatau et al. 2003). However, this convection was short lived and the corresponding wind was weak, therefore, being most likely associated with a bogus monsoon onset (Joseph et al. 2006; Flatau et al. 2003). On the other hand, both the convection and wind were found to rapidly develop into a robust monsoon onset in the second week of June (Joseph et al. 2006).

TABLE 1. Correlation coefficients between forecasts and reanalysis onset dates. Correlations with onset dates issued by IMD are also reported.

		ERA-Interim		
		OCI	HOWI	IMD onset
Forecasts	OCI	0.65*		0.70*
	HOWI		0.52*	0.32**
IMD onset		0.80*	0.73*	

\* Significance at the 5% level.

\*\* Significance at the 10% level.

Overall, both OCI and HOWI results are in good agreement with IMD onset dates, with the OCI displaying a slightly higher correlation (0.80 vs 0.73; Table 1). Earlier- (later-) than-normal onset years, as identified through the lower (upper) terciles of sample distribution, are reported in Fig. 3. In our time series of 17 years, the six lowest onset values are classified as earlier than normal, while the six largest onset values are classified as later-than-normal onset dates (see Fig. 3 for the list of years in each category for each index). OCI and HOWI agree for five of the six early onset years identified in ERA-Interim (Fig. 3). Of the earlier-than-normal onset years in common between OCI and HOWI, only four (i.e., 1990, 1999, 2000, and 2001) correspond to those diagnosed by the IMD criteria. The 1990, 1999, and 2001 are represented among the earliest onset years of the period by all indices. On the other hand, there are some differences in years such as 1991 and 1994 that are identified as normal years using both OCI and HOWI, while have slightly earlier-than-normal ISM onset for IMD.

Later-than-normal onset years identified using OCI exactly agree with the ones using HOWI. Of these six years, four (i.e., 1995, 1997, 2003, and 2004) are also identified as late onsets by IMD classification. 2002 and 1996 have been previously reported as more controversial

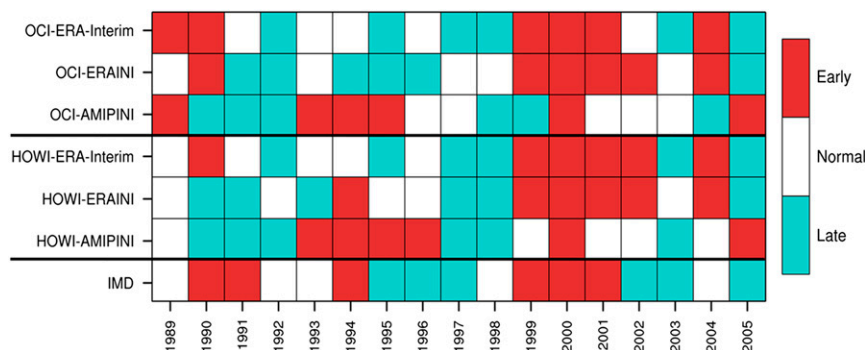


FIG. 3. Years with earlier-than-normal and later-than-normal ISM onset identified both with OCI and HOWI for ERA-Interim and for ERAINI and AMIPINI forecasts. For completeness, early- and late-onset dates as issued by IMD are reported as well.

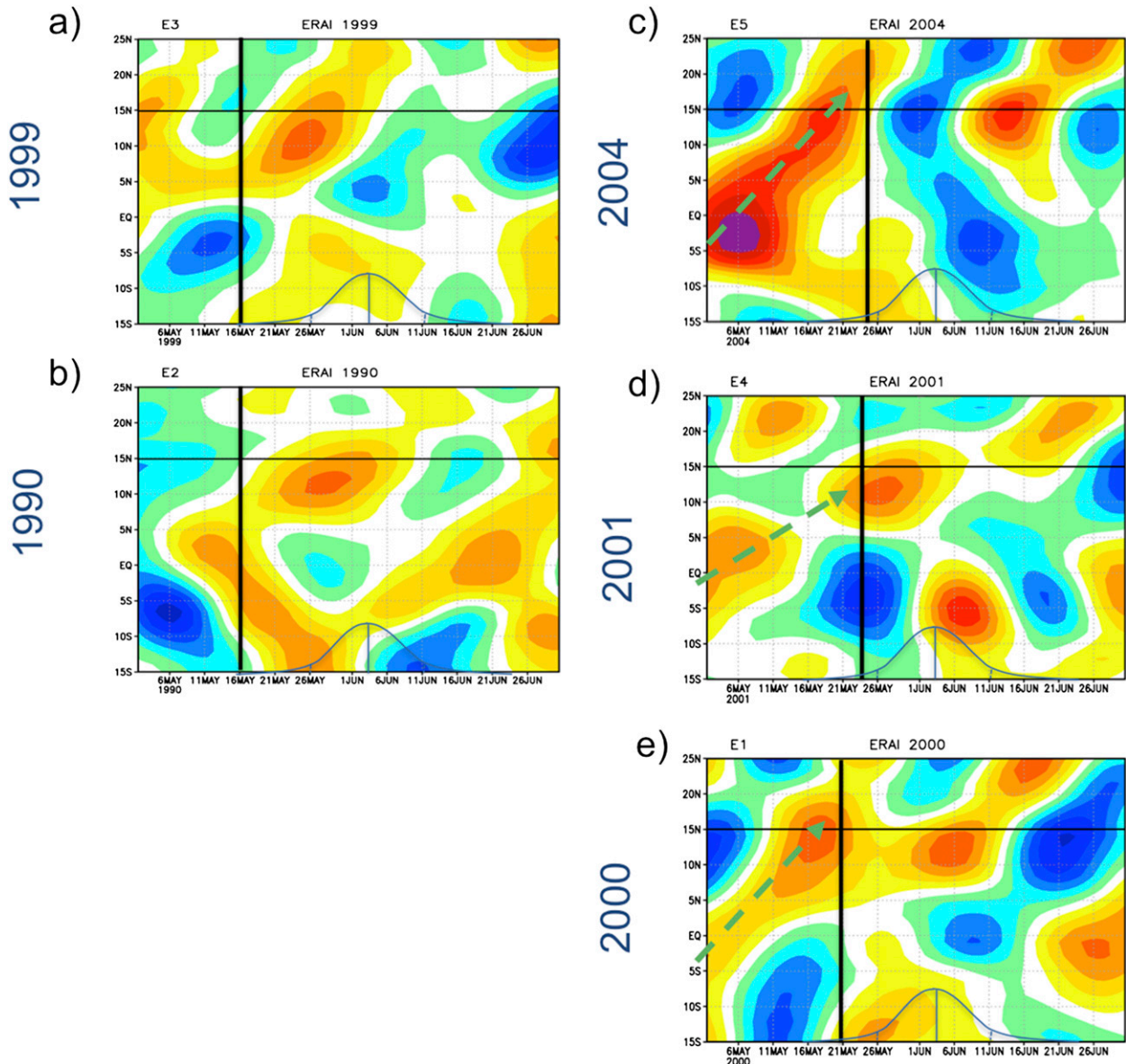


FIG. 4. Time–latitude Hovmöller diagrams of 20–100-day filtered 850-hPa zonal-wind anomalies averaged over  $65^{\circ}$ – $85^{\circ}$ E in ERA-Interim. The years shown have an earlier-than-normal (below lower tercile of sample distribution) monsoon onset date obtained from both OCI and HOWI indices: (a) 1999, (b) 1990, (c) 2004, (d) 2001, and (e) 2000. In (c)–(e), the early monsoon onsets that are triggered by northward-propagating intraseasonal zonal wind anomalies are shown. For each year, the ISM onsets (vertical lines) detected by the OCI are displayed together with the climatological onset distribution.

years (Joseph et al. 2006) and correspond to later-than-normal onsets only when using IMD classification (Fig. 3).

Previous works showed that northward-propagating ISO can modulate the onset of the monsoon (e.g., Krishnamurti and Subrahmanyam 1982; Wang et al. 2009). As discussed in Krishnamurti and Subrahmanyam (1982), the passage of the ISO trough lines over the Indian subcontinent accentuate the monsoon circulation. Therefore, during the developing phase of the monsoon in May, the superposition of an ISO trough anomaly may trigger

earlier-than-normal monsoon onset. Figure 4 shows the time–latitude Hovmöller diagrams of zonal wind daily anomalies at 850 hPa filtered in the 20–100-day band and averaged over  $65^{\circ}$ – $85^{\circ}$ E longitudes. The anomalies are shown for all the five years having an earlier-than-normal monsoon onset according to both OCI and HOWI (the years are 1990, 1999, 2001, 2000, and 2004; see Fig. 3). In 2000, 2001, and 2004, the onset is clearly connected with the passage of the ISO trough over India (Fig. 4, right panels). On the other hand, 1990 and 1999 do not show

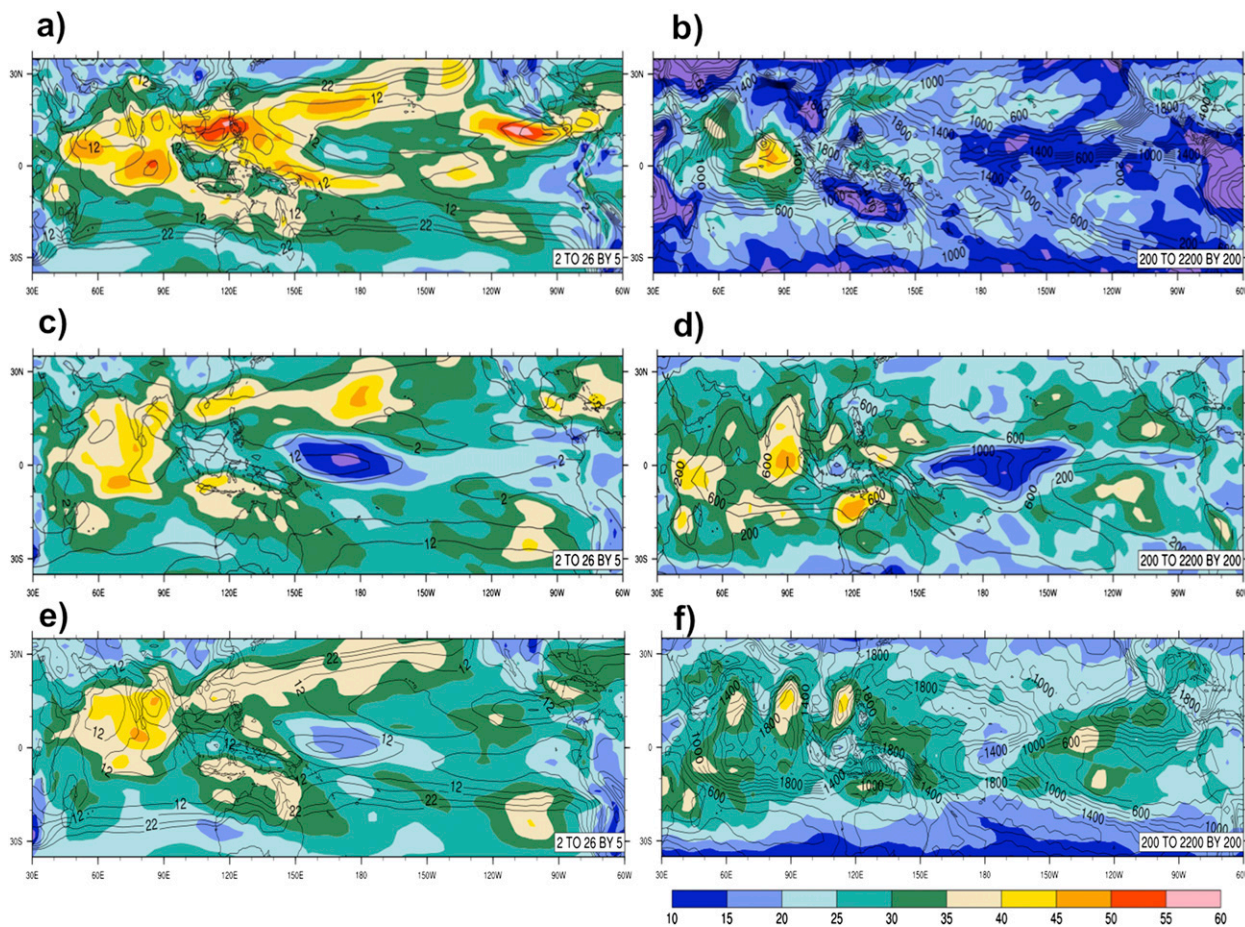


FIG. 5. May–June (MJ) total daily variance (contours) of (a),(c),(e) 850-hPa zonal wind and (b),(d),(f) OLR anomalies for (a),(b) ERA-Interim; (c),(d) ensemble-mean forecasts; and (e),(f) ensemble average of each forecast member variance. The ratio between filtered (20–100 day) and total daily variance is shaded.

signs of northward-propagating ISO during monsoon onset (Fig. 4, left panels).

### 3. Forecasts' performance

The performance of the SSPs implementing the initialization of the atmospheric component using ERA-Interim (ERA-Interim experiment) is reported in terms of the capability of the system in simulating the intraseasonal variability of wind and OLR (section 3a) and of the skill in predicting the ISM onset (section 3b).

#### a. Simulation of intraseasonal variability

Figure 5 compares observed versus forecasted variance of daily 850-hPa zonal wind and OLR anomalies (left and right panels, respectively) during May and June (MJ). Contours show the total daily variance while shading stands for the ratio between intraseasonal (band-pass filtered between 20 and 100 days) and total daily variance. Overall, the ensemble-mean forecasts (Figs. 5c,d)

appear to simulate well the pattern of variability over both Indian and Pacific oceans, in particular in the equatorial band. On the other hand, wind and OLR have lower variability compared to observations (Figs. 5a,b), particularly over subtropical regions. By comparing the variance computed using ensemble-mean forecasts (Figs. 5c,d) with the ensemble average of the variance computed for each forecast member (Figs. 5e,f), it is shown that the discrepancy mentioned above mostly follows from the computation of the ensemble mean, which retains only the variability that is consistent among the forecast ensemble members (predictable signal), therefore, filtering out the noise (Stern and Miyakoda 1995; Alessandri et al. 2011). The variance of the ensemble-mean forecasts (Figs. 5c,d) indicates a considerable predictable signal over the Indian Ocean. Consistently with Stern and Miyakoda (1995), the prediction signal tends to decrease moving poleward from the equator to subtropics. The ratio between filtered (20–100 days) and total daily variance (Fig. 5, shaded) indicates a good

agreement between forecasts and observations. In particular, the ensemble-mean forecasts (Figs. 5c,d) indicate that a considerable component (i.e., more than 35%) of the signal that is predictable over the Indian Ocean is due to intraseasonal variability. Further discussion on the performance of the CMCC SSPS in forecasting intraseasonal variability is being reported in the comparison with the other prediction systems participating in the ISVHE multimodel (Lee et al. 2015; Neena et al. 2014). The comparison of the prediction systems evidences good qualities of the CMCC SSPS in reproducing intraseasonal wind and precipitation anomalies both in winter and summer (Neena et al. 2014; Lee et al. 2015). The analysis going on in the framework of the ISVHE shows that the CMCC SSPS has a good skill in forecasting boreal summer ISOs, which is in line with the other participating models. In particular, the forecasts skill for ISOs is remarkable over northern Indian Ocean, with a considerable performance until lead times of 2–3 weeks (Lee et al. 2015).

#### b. ISM onset skill

The forecasts of the monsoon onset dates defined both through OCI (Fig. 6a) and HOWI (Fig. 6b) show a good skill compared with reanalysis. The ensemble-mean OCI forecasts perform better than HOWI in capturing the respective reanalysis values, with 0.65 correlation (5% significance level) for OCI and 0.52 (5% significance level) for HOWI. Interestingly, the OCI forecasts display an even higher correlation with IMD (0.70, 5% significance level), while HOWI is quite weakly correlated with the onset dates issued by IMD (0.32, not significant at the 5% level).

Both OCI and HOWI perform better for the prediction of early-onset years compared to late-onset years. The ensemble-mean forecasts of the OCI detect five of the six earlier-than-normal onset years in accordance with reanalysis (Fig. 6a; see also Fig. 3). Unlike reanalysis, the forecast of the 2002 monsoon onset using OCI is susceptible to the bogus onset that occurred that year, therefore, identifying an earlier-than-normal onset. Quite similarly to OCI, the HOWI ensemble-mean forecasts can also detect five of the six earlier-than-normal onset years in accordance with reanalysis (Fig. 6b). However, HOWI fails to predict the earlier-than-normal onset of 1990, which is one of the earliest on record for both reanalysis and IMD. In general, the skill for late monsoon onset is very poor. Both OCI and HOWI predict correctly only three out of the six late onset years (Fig. 3).

The probabilistic quality of the forecasts for the dichotomous events of early than normal (occurring in the lower tercile of climatological distribution) and later than

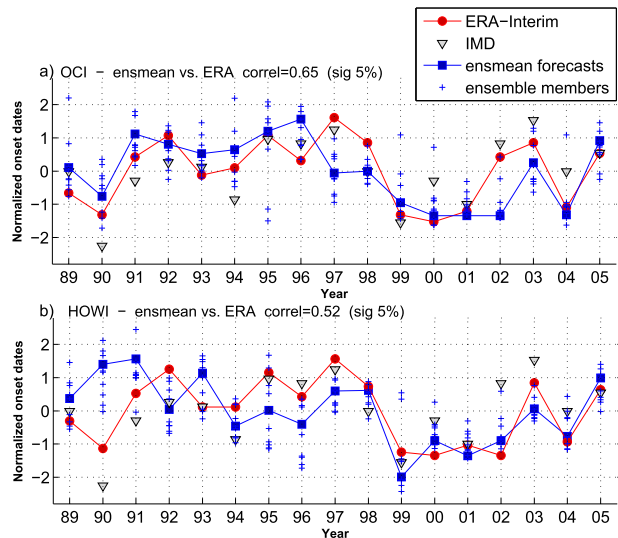


FIG. 6. Normalized onset dates as diagnosed by (a) OCI and (b) HOWI in the forecasts (blue crosses for each member and blue filled squares connected by the blue line for the ensemble means). The normalized dates taken from ERA-Interim are shown as red filled circles connected by the red line. Gray triangles indicate the onset definition by IMD.

normal (upper tercile of the climatological distribution) is summarized in Table 2 in terms of the Brier skill scores (BSS; Wilks 2006). The BSS is a positively oriented scalar measure of the overall accuracy of the probabilistic forecasts displaying 1.0 as the maximum value and takes the climatological forecasts as the reference corresponding to no skill (zero score), while negative values stand for forecasts performing worse than climatological information. The prediction of earlier-than-normal monsoon onset is shown to have considerable probabilistic performance for both OCI and HOWI (Table 2, first row). In particular, OCI has a larger BSS than HOWI (0.43 vs 0.34). The prediction of later-than-normal monsoon onsets displays very poor performance with a positive but very small BSS for OCI. HOWI is not useful for late-onset prediction being worse than climatological forecasts as indicated by the negative BSS.

#### 4. Forecasts' sensitivity to the initialization of the atmosphere

To assess the effect of the realistic initialization of the atmosphere on the prediction skill, we compare the forecasts initialized from ERA-Interim (ERAINI) with a set of predictions performed with atmospheric IC taken from an AMIP-type simulation (AMIPINI experiment; see section 2a). ERAINI significantly (5% significance level) improves the BSS for the forecasts of early monsoon onsets compared to AMIPINI (Fig. 7a, left). In contrast, the inclusion of realistic atmospheric

TABLE 2. Forecasts probabilistic performance in terms of Brier skill score for earlier-than-normal and later-than-normal ISM onset dates identified using OCI and HOWI for both ERAINI and AMIPINI experiments.

	Expt	OCI	HOWI
Earlier-than-normal onset	ERAINI	0.43	0.34
	AMIPINI	0.18	−0.03
Later-than-normal onset	ERAINI	0.02	−0.24
	AMIPINI	−0.17	−0.13

initial conditions does not positively affect the prediction of late monsoon onsets (Fig. 7a, right). To assess the overall terciles performance of the forecasts as recommended by the World Meteorological Organization (WMO 2010; Gerrity 1992), Fig. 7b also reports the Gerrity skill score [or a Gandin–Murphy skill score (GMSS)] as described in Lee and Seo (2013). The GMSS for OCI prediction is enhanced considerably in ERAINI compared to AMIPINI, with a significant (5% level of significance) increase from 0.30 to 0.66 (note that GMSS has a maximum value of 1). On the other hand, the comparison of the GMSS between ERAINI and AMIPINI shows only a little improvement for HOWI (from 0.27 to 0.39; the increase is not significant at 5% level).

The transition toward the monsoon onset typically shows the reinforcement of the circulation to the southwest

of India coupled with enhanced moisture transport to the convection area over equatorial Bay of Bengal (Wang and Fan 1999; Figs. 8a–c). In AMIPINI, the southerly component of Somali jet is stronger than observed. Therefore, the moisture transport is directed mostly north into the Arabian Sea, while the component staying south of the Indian subcontinent and feeding the equatorial westerly circulation is too small. This leads to a biased equatorial westerly circulation and a too weak moisture transport from the Somali jet to the eastern equatorial Bay of Bengal (Figs. 8g–i). By one hand, the northward shift reduces moisture transport by equatorial southwesterly circulation to support convection over the eastern equatorial Bay of Bengal (Ding and Sikka 2006; Yu et al. 2012). On the other hand, the lowered tropical convective heat source over the Bay of Bengal may further abate the portion of equatorial westerlies that are heat induced according to the analytic model of tropical response by Gill (1980). The bias described leads to a systematic premature onset of the ISM in AMIPINI (Figs. 8g–i). The climatological onset date in AMIPINI (horizontal dashed green line in Fig. 9a) is 26 May when detected by the OCI and 20 May when using the HOWI (Fig. 9b). Compared to ERA-Interim (horizontal dashed red lines in Fig. 9), this means an averaged premature onset by 7 and 10 days, respectively. In contrast, ERAINI shows a more realistic climatological

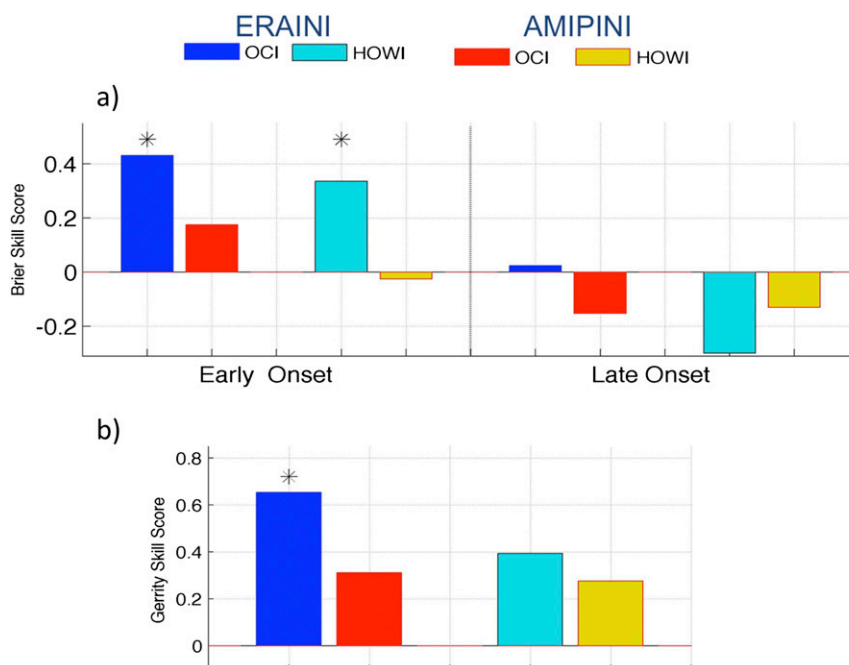


FIG. 7. (a) Brier skill score for the forecast of the dichotomous events of early (left bars) and late (right bars) monsoon onset. (b) Gerrity skill score summarizing overall terciles performance. Asterisks indicate if the value is significantly enhanced compared to the other experiment (5% level; Monte Carlo method).

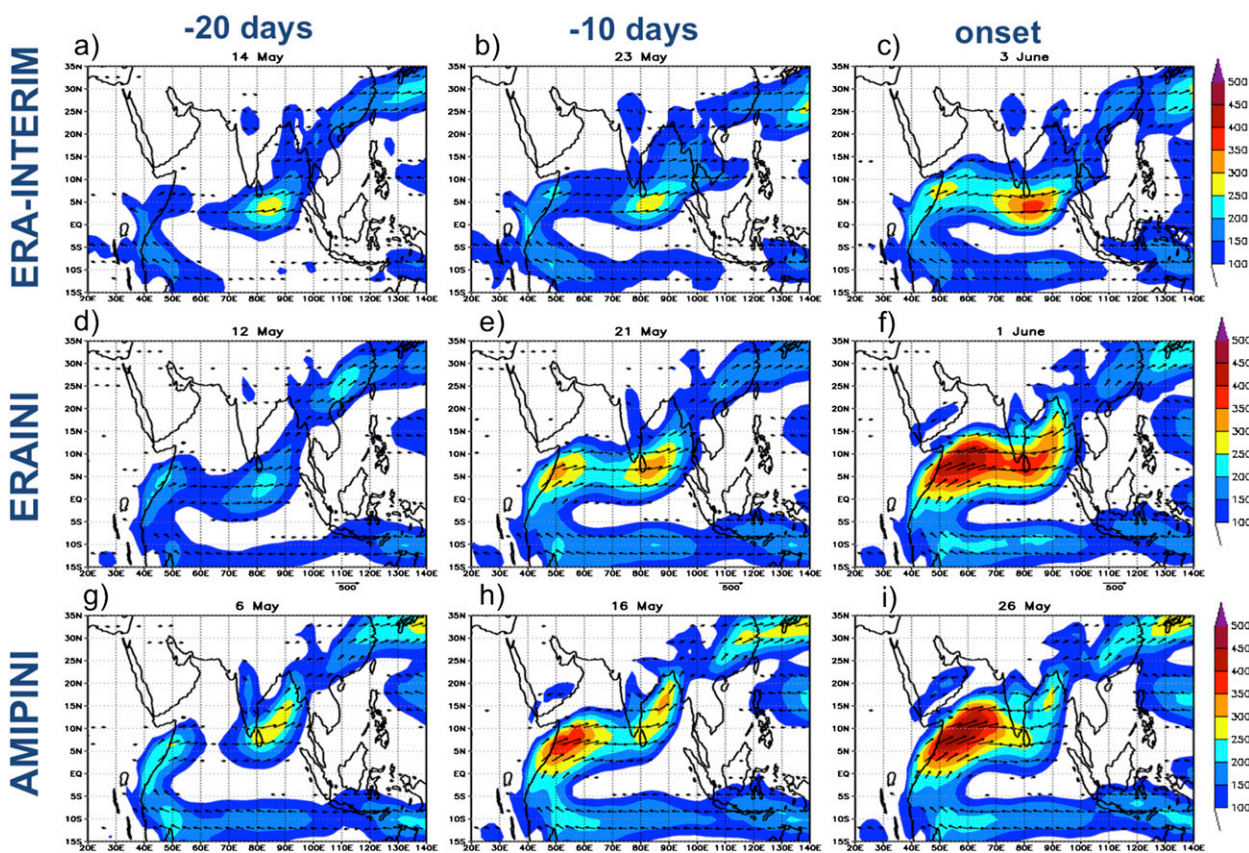


FIG. 8. Climatological 10-day-averaged vertically integrated moisture transport [ $\text{kg (m s)}^{-1}$ ; the intensity is shaded] centered on (a),(d),(g) -20 days; (b),(e),(h) -10 days; and (c),(f),(i) climatological onset date for (top) ERA-Interim, (middle) ERAINI, and (bottom) AMIPINI.

onset sequence during May (Figs. 8d,e) due to the better representation of the atmospheric mean state in the IC. This leads to an averaged onset date in ERAINI much closer to ERA-Interim for both OCI (1 June in ERAINI vs 3 June in ERA-Interim; Fig. 9a) and HOWI (26 May vs 30 May; Fig. 9b). As is clear from Figs. 8c,f,i, the beneficial effect of realistic initialization on the climatological onset transition is no longer perceptible after the end of May. In fact, by early June the bias in ERAINI (Fig. 8f) converges to the same values of the forecasts where the atmospheric model is not initialized with reanalysis (not shown). Therefore, the better climatological monsoon onset sequence due to the realistic atmospheric initialization in ERAINI can hardly influence the prediction of late-onset events by comparison with AMIPINI.

As discussed in section 2c(3), early monsoon onset in some years are clearly connected with the northward propagation of ISO anomalies from the equatorial Indian Ocean to the Indian subcontinent. In particular, our analysis performed on the reanalysis data shows that the early onsets in 2000, 2001, and 2004 are triggered by the

passage of ISO troughs over India (Figs. 10a-c). This is well represented in ERAINI, which well captures the in-phase northward propagation of the initialized ISO anomalies over the equatorial Indian Ocean (Figs. 10d-f). The realistic phase initialization in ERAINI and the capability of the coupled model to propagate northward the ISO anomalies appear to initiate the earlier-than-normal monsoons of 2000, 2001, and 2004 in accordance with the reanalysis (Figs. 10a-c). Consistently, AMIPINI do not represent realistic initialization of intraseasonal variability, thus failing to represent the earlier-than-normal onset of the monsoon in those years (Figs. 10g-i). The only exception is 2000, when a very early onset is detected but for a different reason. In fact, the early AMIPINI onset in 2000 is due to a nonpropagating synoptic system anomalously persisting on the Indian subcontinent. Quite interestingly, as shown in Fig. 10g, AMIPINI shows the northward-propagating ISO in 2004. However, this ISO anomaly in AMIPINI develops out of phase compared with the reanalysis (Fig. 10a), therefore, being connected with a normal onset for 2004 instead of an early one.

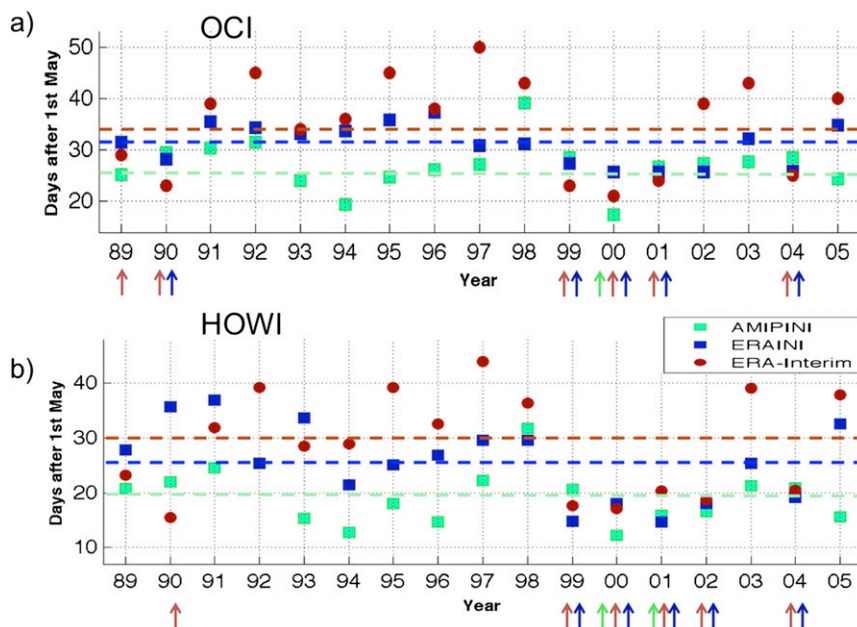


FIG. 9. Onset dates (in days after 1st May) as diagnosed by (a) OCI and (b) HOWI for ERAINI (in blue) and AMIPINI (in green) forecasts and for ERA-Interim (in red). Red arrows on the  $x$  axis indicate early (lower tercile) onset dates in the reanalysis. Blue and green arrows indicate if the model is able to forecast early onset according to reanalysis. Horizontal dashed lines indicate climatological onset dates.

## 5. Discussion and conclusions

The subseasonal forecasts performed with the CMCC prediction system implementing a realistic initialization of the atmospheric component from ERA-Interim (ERAINI experiment) shows a considerable skill in predicting, one month in advance, the onset of the ISM. The forecasts of ISM onset based on both circulation (OCI) and hydrological (HOWI) indices show some skill, albeit the OCI prediction has a better correlation (0.65 vs 0.52; 5% significance level) with the reanalysis counterpart. The probabilistic forecasts display the ability to predict earlier-than-normal (before lower tercile of the sample distribution) monsoon onsets. The OCI performs better with a BSS of 0.43 versus 0.34 for HOWI. On the other hand, the prediction of later-than-normal onsets (i.e., after upper tercile of the sample distribution) displays a very weak overall performance with a positive but very small BSS for OCI and a negative BSS for HOWI.

The realistic initialization of the atmospheric component significantly contributes to the prediction skill of an earlier-than-normal monsoon onset. Compared with the forecasts initialized from the AMIP-type simulations (AMIPINI experiment), the probabilistic prediction of an earlier-than-normal monsoon onset is improved significantly (5% level of significance) using both OCI (BSS of 0.43 vs 0.18) and HOWI (BSS of 0.34 vs  $-0.03$ ).

Our results indicate that the improved predictability of early onsets of the ISM may follow at least in part from the better representation of the atmospheric mean state in the ICs of ERAINI. In fact, the realistic initialization is able to correct the bias of the atmospheric model that affects AMIPINI leading to a systematically premature ISM onset.

Our analysis of the intraseasonal variability of ERA-Interim has shown that a northward-propagating ISO may affect the onset of the monsoon in some years and that the earlier-than-normal onsets in 2000, 2001, and 2004 appear clearly triggered by the passage of the ISO trough over India. The realistic 1 May phase initialization of ISO anomalies in ERAINI over the equatorial Indian Ocean and the subsequent capability of the coupled model to propagate them northward, appears linked to the earlier-than-normal monsoon onset of 2000, 2001, and 2004 in accordance with reanalysis. This drives a more realistic evolution of intraseasonal anomalies in ERAINI compared to AMIPINI leading to a consistently improved prediction of the earlier-than-normal monsoon onset.

The prediction of late onsets is not noticeably improved by the realistic atmospheric initialization. This is at least in part due to the fact that the beneficial effect on the atmosphere biases and the representation of ISO anomalies is limited to the first month of forecasts. Our results show that the effect of realistic atmosphere

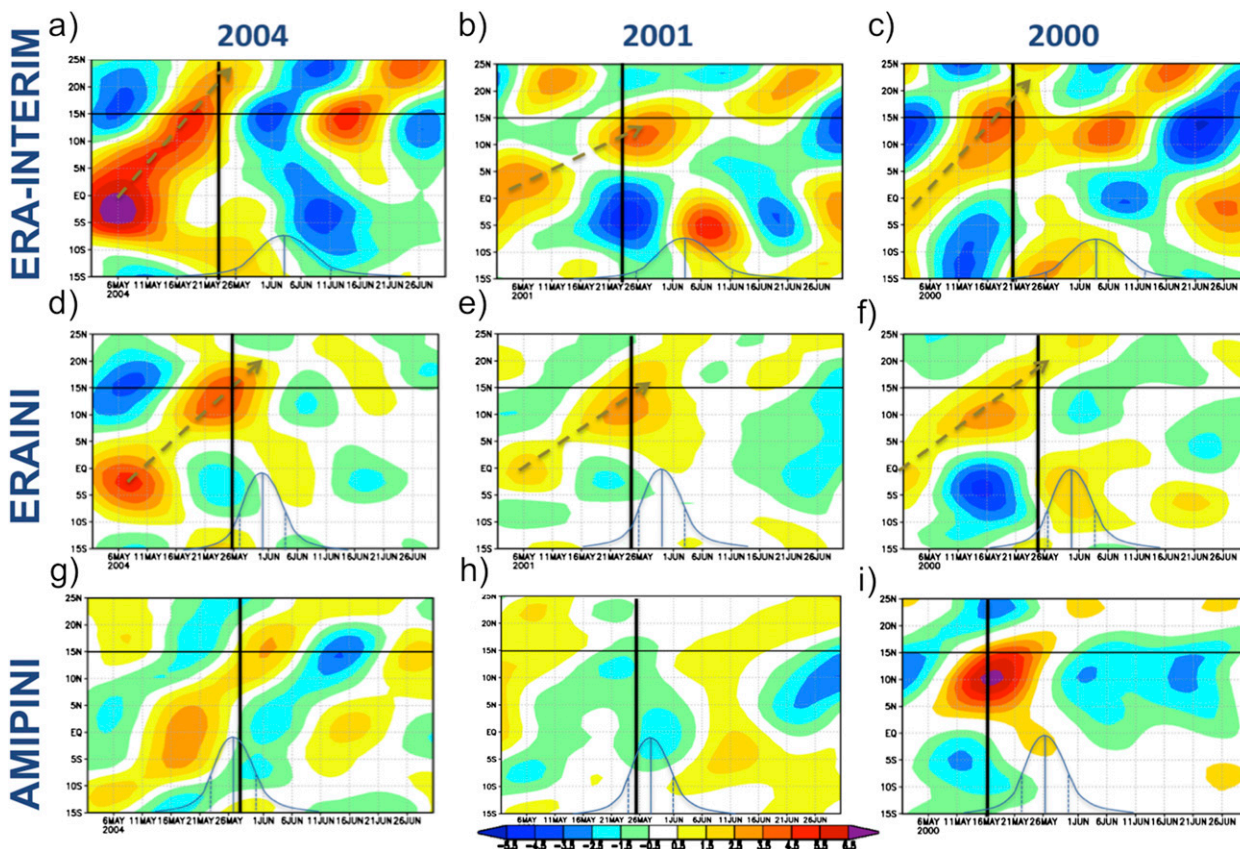


FIG. 10. Time–latitude plots of 20–100-day filtered 850-hPa zonal-wind anomalies (shaded) averaged over a longitudinal band of 65°–85°E. The three observed early monsoon onset that are triggered by northward-propagating intraseasonal zonal wind anomalies, according to Fig. 4, are shown for (top) ERA-Interim, (middle) ERAINI, and (bottom) AMIPINI forecasts. For each year, the ISM onsets (vertical lines) detected by the OCI are displayed together with the climatological onset distribution.

initialization on the climatological onset transition is no longer perceptible by early June. Furthermore, the predictability of intraseasonal variability is currently limited to a maximum lead time of 3–4 weeks (Fu et al. 2011; Lee et al. 2015). Therefore, the late onset of the monsoon, occurring after week 6 from the start date, is too far away from the initial time to be influenced by the improved subseasonal transition or by the initialized intraseasonal anomalies. On the other hand, it is observed that the speed of meridional propagation of the intraseasonal modes is around  $0.75^\circ$  latitude per day (Krishnamurti and Subrahmanyam 1982). The northward-propagating modes initialized around the equator on 1 May will have traveled well beyond the Indian subcontinent by the end of the month, so can hardly influence the onset of the monsoon at later stages. Other external forcing like El Niño and the Indian Ocean dipole influence the monsoon onset dates (Joseph et al. 1994; Sankar et al. 2011), and they should be investigated to fully understand the weaker skill for late monsoon onset prediction. Recent studies, for example,

have shown that Pacific Ocean SST biases may lead to unrealistic onset dates in fully coupled models (Prodhomme et al. 2014). In our seasonal prediction system, the bias in the tropical Pacific is smaller than  $0.2^\circ\text{C}$  during the first month of the forecast but it tends to increase beyond  $0.5^\circ\text{C}$  in the second month (Alessandri et al. 2010; Borrelli et al. 2012). The increased SST bias in the tropical Pacific at 1-month lead could then affect delayed onsets, reducing the prediction skill. The effect of SST biases on the skill of ISM onset prediction will be further investigated in future works.

The results of this study concern the effects of realistic initialization of the atmosphere on the prediction of Indian summer monsoon onset. We believe that the effect on the prediction of the assimilation of observed data to initialize the ocean is also a very important topic. Future works will address the sensitivity of the skill in predicting ISM onset to the initialization of the ocean component. To this aim, an ad hoc set of retrospective forecasts initialized with and without ocean data

assimilation will be performed when adequate computing resources become available.

Previous literature also documented the importance of ocean–atmosphere coupling for the simulation of the intraseasonal variability of the Asian summer monsoon (Xavier et al. 2007) and for the skill of monthly forecasts to predict June rainfall over India (Vitart and Molteni 2009), therefore, indicating that atmosphere–ocean coupling may play a role in the onset of the ISM. In this regard, the exercise of comparing SST-forced and coupled model experiments has been widely used in literature to evaluate the effects of atmosphere–ocean coupling, and for the Indian monsoon it has already been considered for the predictability discussion (Cherchi and Navarra 2013), and for understanding the factors influencing the monsoon onset (Prodhomme et al. 2014). Future works will address the contribution from ocean–atmosphere coupling to the skill in predicting ISM onset. To this aim, the design of a set of retrospective forecasts to be performed in both coupled and SST forced mode is under evaluation.

**Acknowledgments.** This work was partially supported by the European Union Seventh Framework Programme (FP7/2007-13) under Grant 303208 (CLIMITS Project) and under Grant 308378 (SPECS Project). AC, AB, SM, and AN acknowledge the financial support of the Italian Ministry of Education, University and Research, and Ministry for Environment, Land and Sea through the project GEMINA and that of FP7/2007-13 INDO-MARECLIM Project (Grant 295092). JYL and BW were supported by the National Research Foundation of Korea through a Global Research Laboratory (GRL) Grant (MEST 2011-0021927). Special thanks to P.V. Joseph for his advice on the skill of empirical prediction schemes presented in previous literature.

## REFERENCES

- Alessandri, A., 2006: Effects of land surface and vegetation processes on the climate simulated by an atmospheric general circulation model. Ph.D. thesis in Geophysics, Bologna University Alma Mater Studiorum, Bologna, Italy, 114 pp.
- , S. Gualdi, J. Polcher, and A. Navarra, 2007: Effects of land surface–vegetation on the boreal summer surface climate of a GCM. *J. Climate*, **20**, 255–277, doi:[10.1175/JCLI3983.1](https://doi.org/10.1175/JCLI3983.1).
- , A. Borrelli, S. Masina, P. D. Pietro, A. F. Carril, A. Cherchi, S. Gualdi, and A. Navarra, 2010: The CMCC-INGV Seasonal Prediction System: Improved ocean initial conditions. *Mon. Wea. Rev.*, **138**, 2930–2952, doi:[10.1175/2010MWR3178.1](https://doi.org/10.1175/2010MWR3178.1).
- , —, A. Navarra, A. Arribas, M. Déqué, P. Rogel, and A. Weisheimer, 2011: Evaluation of probabilistic quality and value of the ENSEMBLES multimodel seasonal forecasts: Comparison with DEMETER. *Mon. Wea. Rev.*, **139**, 581–607, doi:[10.1175/2010MWR3417.1](https://doi.org/10.1175/2010MWR3417.1).
- , P. Fogli, M. Vichi, and N. Zeng, 2012: Strengthening of the hydrological cycle in future scenarios: Atmospheric energy and water balance perspective. *Earth Syst. Dyn.*, **3**, 199–212, doi:[10.5194/esd-3-199-2012](https://doi.org/10.5194/esd-3-199-2012).
- Andersson, E., and J.-N. Thépaut, 2008: ECMWFs 4D-Var data assimilation system—The genesis and ten years in operations. *ECMWF Newsletter*, No. 115, ECMWF, Reading, United Kingdom, 8–12.
- Bellucci, A., S. Masina, P. D. Pietro, and A. Navarra, 2007: Using temperature–salinity relations in a global ocean implementation of a multivariate data assimilation scheme. *Mon. Wea. Rev.*, **135**, 3785–3807, doi:[10.1175/2007MWR1821.1](https://doi.org/10.1175/2007MWR1821.1).
- Berrisford, P., D. Dee, K. Fielding, M. Fuentes, P. Kallberg, S. Kobayashi, and S. Uppala, 2009: The ERA-Interim archive. Tech. ERA Rep. Series 1, ECMWF, Reading, United Kingdom, 16 pp.
- Borrelli, A., S. Masina, A. Bellucci, A. Alessandri, and S. Gualdi, 2012: Seasonal Prediction System at CMCC. CMCC Tech. Rep., CMCC, 18 pp.
- Cherchi, A., and A. Navarra, 2003: Reproducibility and predictability of the Asian summer monsoon in the ECHAM4-GCM. *Climate Dyn.*, **20**, 365–379, doi:[10.1007/s00382-002-0280-6](https://doi.org/10.1007/s00382-002-0280-6).
- , and —, 2013: Influence of ENSO and of the Indian Ocean Dipole on the Indian summer monsoon variability. *Climate Dyn.*, **41**, 81–103, doi:[10.1007/s00382-012-1602-y](https://doi.org/10.1007/s00382-012-1602-y).
- Dee, D., and Coauthors, 2011: The ERA-Interim reanalysis: Conguration and performance of the data assimilation system. *Quart. J. Roy. Meteor. Soc.*, **137**, 553–597, doi:[10.1002/qj.828](https://doi.org/10.1002/qj.828).
- Ding, Y., and D. Sikka, 2006: Synoptic systems and weather. *The Asian Monsoon*, B. Wang, Ed., Springer, 131–201.
- DiPietro, P., and S. Masina, 2009: The CMCC-INGV global ocean data assimilation system (CIGODAS). Tech. Rep. RP0071, Centro Euro-Mediterraneo per i Cambiamenti Climatici, 39 pp.
- Fasullo, J., and P. Webster, 2003: A hydrological definition of Indian monsoon onset and withdrawal. *J. Climate*, **16**, 3200–3211, doi:[10.1175/1520-0442\(2003\)016<3200a:AHDOIM>2.0.CO;2](https://doi.org/10.1175/1520-0442(2003)016<3200a:AHDOIM>2.0.CO;2).
- Flatau, M., P. Flatau, and D. Rudnick, 2001: The dynamics of double monsoon onsets. *J. Climate*, **14**, 4130–4146, doi:[10.1175/1520-0442\(2001\)014<4130:TDODMO>2.0.CO;2](https://doi.org/10.1175/1520-0442(2001)014<4130:TDODMO>2.0.CO;2).
- , —, J. Schmidt, and G. Kiladis, 2003: Delayed onset of the 2002 Indian monsoon. *Geophys. Res. Lett.*, **30**, 1768–1771, doi:[10.1029/2003GL017434](https://doi.org/10.1029/2003GL017434).
- Fogli, P., and Coauthors, 2009: INGV-CMCC carbon (ICC): A carbon cycle Earth system model. CMCC Tech. Rep. RP0061, CMCC, 31 pp. [Available online at <http://www.cmcc.it/publications-meetings/publications/research-papers/rp0061-ingv-cmcc-carbon-icc-a-carbon-cycle-earth-system-model>.]
- Fu, X., B. Wang, Q. Bao, P. Liu, and J.-Y. Lee, 2009: Impacts of initial conditions on monsoon intraseasonal forecasting. *Geophys. Res. Lett.*, **36**, L08801, doi:[10.1029/2009GL037166](https://doi.org/10.1029/2009GL037166).
- , —, J.-Y. Lee, W. Wang, and L. Gao, 2011: Sensitivity of dynamical intraseasonal prediction skill to different initial conditions. *Mon. Wea. Rev.*, **139**, 2572–2592, doi:[10.1175/2011MWR3584.1](https://doi.org/10.1175/2011MWR3584.1).
- , J.-Y. Lee, B. Wang, W. Wang, and F. Vitart, 2013: Intraseasonal forecasting of Asian summer monsoon in four operational and research models. *J. Climate*, **26**, 4186–4203, doi:[10.1175/JCLI-D-12-00252.1](https://doi.org/10.1175/JCLI-D-12-00252.1).
- Gadgil, S., and S. Sajani, 1998: Monsoon precipitation in the AMIP runs. *Climate Dyn.*, **14**, 659–689, doi:[10.1007/s003820050248](https://doi.org/10.1007/s003820050248).
- Gerrity, J. P., Jr., 1992: A note on Gandin and Murphy's equitable skill score. *Mon. Wea. Rev.*, **120**, 2709–2712, doi:[10.1175/1520-0493\(1992\)120<2709:ANOGAM>2.0.CO;2](https://doi.org/10.1175/1520-0493(1992)120<2709:ANOGAM>2.0.CO;2).

- Gill, A. E., 1980: Some simple solutions for heat-induced tropical circulation. *Quart. J. Roy. Meteor. Soc.*, **106**, 447–462, doi:[10.1002/qj.49710644905](https://doi.org/10.1002/qj.49710644905).
- Goswami, B., 2005: South Asian summer monsoon: An overview. *The Global Monsoon System: Research and Forecast*, C. Chang, B. Wang, and N. Lau, Eds., WMO Tech. Doc. 1266, 28 pp.
- , J. Kulkarni, V. Mujumdar, and R. Chattopadhyay, 2010: On factors responsible for recent secular trend in the onset phase of monsoon intraseasonal oscillations. *Int. J. Climatol.*, **30**, 2240–2246, doi:[10.1002/joc.2041](https://doi.org/10.1002/joc.2041).
- India Meteorological Department, 1943: *Climatological Atlas for Airman*. India Meteorological Department, 100 pp.
- Joseph, P., J. Eischeid, and R. Pyle, 1994: Interannual variability of the onset of the Indian summer monsoon and its association with atmospheric features, El Niño, and sea surface temperature anomalies. *J. Climate*, **7**, 81–105, doi:[10.1175/1520-0442\(1994\)007<0081:IVOTOO>2.0.CO;2](https://doi.org/10.1175/1520-0442(1994)007<0081:IVOTOO>2.0.CO;2).
- , K. Sooraj, and C. Rajan, 2006: The summer monsoon onset process over South Asia and an objective method for the date of monsoon onset over Kerala. *Int. J. Climatol.*, **26**, 1871–1893, doi:[10.1002/joc.1340](https://doi.org/10.1002/joc.1340).
- Ju, J., and J. Slingo, 1995: The Asian summer monsoon and ENSO. *Quart. J. Roy. Meteor. Soc.*, **121**, 1133–1168, doi:[10.1002/qj.49712152509](https://doi.org/10.1002/qj.49712152509).
- Kang, I. S., and Coauthors, 2002: Intercomparison of the climatological variations of Asian summer monsoon precipitation simulated by 10 GCMs. *Climate Dyn.*, **19**, 383–395, doi:[10.1007/s00382-002-0245-9](https://doi.org/10.1007/s00382-002-0245-9).
- Kirchner, I., 2001: The INTER handbook. Tech. Rep., Max-Planck-Institut für Meteorologie. Hamburg, Germany, 20 pp.
- Krishnamurthy, P., and J. Shukla, 2011: Predictability of the Indian monsoon in coupled general circulation models. COLA Tech. Rep., July 2011, 45 pp.
- Krishnamurti, T., 1985: Summer Monsoon Experiment—A review. *Mon. Wea. Rev.*, **113**, 1590–1626, doi:[10.1175/1520-0493\(1985\)113<1590:SMER>2.0.CO;2](https://doi.org/10.1175/1520-0493(1985)113<1590:SMER>2.0.CO;2).
- , and D. Subrahmanyam, 1982: The 30–50 day mode at 850 mb during MONEX. *J. Atmos. Sci.*, **39**, 2088–2095, doi:[10.1175/1520-0469\(1982\)039<2088:TDMAMD>2.0.CO;2](https://doi.org/10.1175/1520-0469(1982)039<2088:TDMAMD>2.0.CO;2).
- Lee, J.-Y., and Coauthors, 2010: How are seasonal prediction skills related to models' performance on mean state and annual cycle? *Climate Dyn.*, **35**, 267–283, doi:[10.1007/s00382-010-0857-4](https://doi.org/10.1007/s00382-010-0857-4).
- , B. Wang, M. Wheeler, X. Fu, D. Waliser, and I. Kang, 2013: Real-time multivariate indices for the boreal summer intraseasonal oscillation over the Asian monsoon region. *Climate Dyn.*, **40**, 493–509, doi:[10.1007/s00382-012-1544-4](https://doi.org/10.1007/s00382-012-1544-4).
- Lee, S.-E., and K.-H. Seo, 2013: The development of a statistical forecast model for Changma. *Wea. Forecasting*, **28**, 1304–1321, doi:[10.1175/WAF-D-13-00003.1](https://doi.org/10.1175/WAF-D-13-00003.1).
- Lee, S.-S., J.-Y. Lee, K.-J. Ha, B. Wang, J. Kyung, and E. Schemm, 2011: Deficiencies and possibilities for long-lead coupled climate prediction of the western North Pacific-East Asian summer monsoon. *Climate Dyn.*, **36**, 1173–1188, doi:[10.1007/s00382-010-0832-0](https://doi.org/10.1007/s00382-010-0832-0).
- , B. Wang, D. E. Waliser, J. M. Neena, and J.-Y. Lee, 2015: Predictability and prediction skill of the boreal summer intraseasonal oscillation in the Intraseasonal Variability Hindcast Experiment. *Climate Dyn.*, in press.
- Li, J., and L. Zhang, 2009: Wind onset and withdrawal of Asian summer monsoon and their simulated performance in AMIP models. *Climate Dyn.*, **32**, 935–968, doi:[10.1007/s00382-008-0465-8](https://doi.org/10.1007/s00382-008-0465-8).
- Liebmann, B., and C. Smith, 1996: Description of a complete (interpolated) outgoing longwave radiation dataset. *Bull. Amer. Meteor. Soc.*, **77**, 1275–1277.
- Maded, G., P. Delecluse, M. Imbard, and C. Levy, 1998: OPA version 8.1 Ocean General Circulation Model reference manual. Tech. Rep. Note 11, LODYC/IPSL, 91 pp.
- Masina, S., P. di Pietro, A. Storto, and A. Navarra, 2011: Global ocean re-analyses for climate applications. *Dyn. Atmos. Oceans*, **52**, 341–366, doi:[10.1016/j.dynatmoce.2011.03.006](https://doi.org/10.1016/j.dynatmoce.2011.03.006).
- Materia, S., A. Borrelli, A. Bellucci, A. Alessandri, P. Di Pietro, P. Athanasiadis, A. Navarra, and S. Gualdi, 2014: Impact of atmosphere and land surface initial conditions on seasonal forecasts of global surface temperature. *J. Climate*, **27**, 9253–9271, doi:[10.1175/JCLI-D-14-00163.1](https://doi.org/10.1175/JCLI-D-14-00163.1).
- Neena, J., J.-Y. Lee, D. Waliser, B. Wang, and X. Jiang, 2014: Predictability of the Madden-Julian oscillation in the Intraseasonal Variability Hindcast Experiment (ISVHE). *J. Climate*, **27**, 4531–4543, doi:[10.1175/JCLI-D-13-00624.1](https://doi.org/10.1175/JCLI-D-13-00624.1).
- Pai, D. S., and R. M. Nair, 2009: Summer monsoon onset over Kerala: New definition and prediction. *J. Earth Syst. Sci.*, **118**, 123–135, doi:[10.1007/s12040-009-0020-y](https://doi.org/10.1007/s12040-009-0020-y).
- Palmer, T., and Coauthors, 2004: Development of a European Multimodel Ensemble System for Seasonal-to-Interannual Prediction (DEMETER). *Bull. Amer. Meteor. Soc.*, **85**, 853–872, doi:[10.1175/BAMS-85-6-853](https://doi.org/10.1175/BAMS-85-6-853).
- Parthasarathy, B., A. Munot, and D. Kothwale, 1994: All-India monthly and seasonal rainfall series: 1871–1993. *Theor. Appl. Climatol.*, **49**, 217–224, doi:[10.1007/BF00867461](https://doi.org/10.1007/BF00867461).
- Pearce, R., and U. Mohanty, 1984: Onsets of the Asian summer monsoon 1979–82. *J. Atmos. Sci.*, **41**, 1620–1639, doi:[10.1175/1520-0469\(1984\)041<1620:OOTASM>2.0.CO;2](https://doi.org/10.1175/1520-0469(1984)041<1620:OOTASM>2.0.CO;2).
- Preethi, B., R. Kripalani, and K. Kumar, 2010: Indian summer monsoon rainfall variability in global coupled ocean-atmospheric models. *Climate Dyn.*, **35**, 1521–1539, doi:[10.1007/s00382-009-0657-x](https://doi.org/10.1007/s00382-009-0657-x).
- Prodhomme, C., P. Terray, S. Masson, G. Boschat, and T. Izumo, 2014: Oceanic factors controlling the Indian summer monsoon onset in a coupled model. *Climate Dyn.*, doi:[10.1007/s00382-014-2200-y](https://doi.org/10.1007/s00382-014-2200-y), in press.
- Rajeevan, M., and R. Nanjundiah, 2009: Coupled model simulations of twentieth century climate of the Indian summer monsoon. *Current Trends in Science*, N. Mukunda, Ed., Indian Academy of Sciences, 537–568.
- , C. Unnikrishnan, and B. Preethi, 2012: Evaluation of the ENSEMBLES multi-model seasonal forecasts of Indian summer monsoon variability. *Climate Dyn.*, **38**, 2257–2274, doi:[10.1007/s00382-011-1061-x](https://doi.org/10.1007/s00382-011-1061-x).
- Rayner, N., D. Parker, E. Horton, C. Folland, L. Alexander, D. Rowell, E. Kent, and A. Kaplan, 2003: Global analysis of sea surface temperature, sea ice, and night marine air temperature since the late nineteenth century. *J. Geophys. Res.*, **108**, 4407, doi:[10.1029/2002JD002670](https://doi.org/10.1029/2002JD002670).
- Roeckner, E., and Coauthors, 1996: The atmospheric general circulation model ECHAM-4: Model description and simulation of present-day climate. Tech. Rep. 218, Max-Planck-Institut für Meteorologie, 94 pp.
- , and Coauthors, 2003: The atmospheric general circulation model ECHAM5. Part I: Model description. Tech. Rep. 349, Max-Planck-Institut für Meteorologie, Hamburg, Germany, 127 pp.
- , and Coauthors, 2006: Sensitivity of simulated climate to horizontal and vertical resolution in the ECHAM5 atmosphere model. *J. Climate*, **19**, 3771–3791, doi:[10.1175/JCLI3824.1](https://doi.org/10.1175/JCLI3824.1).

- Sankar, S., M. R. Kumar, and C. Reason, 2011: On the relative roles of El Niño and Indian Ocean dipole events on the monsoon onset over Kerala. *Theor. Appl. Climatol.*, **103**, 359–374, doi:[10.1007/s00704-010-0306-7](https://doi.org/10.1007/s00704-010-0306-7).
- Scoccimarro, E., S. Gualdi, A. Bellucci, A. Carril, P. Fogli, and A. Navarra, 2007: CMCC-SXF025: A high-resolution coupled atmosphere ocean general circulation climate model. Tech. Rep. 18, Centro Euro-Mediterraneo per i Cambiamenti Climatici, 63 pp.
- Seo, K.-H., J. Schemm, W. Wang, and A. Kumar, 2007: The boreal summer intraseasonal oscillation simulated in the NCEP climate forecast system: The effect of sea surface temperature. *Mon. Wea. Rev.*, **135**, 1807–1827, doi:[10.1175/MWR3369.1](https://doi.org/10.1175/MWR3369.1).
- Soman, M., and K. K. Kumar, 1993: Space–time evolution of meteorological features associated with the onset of the Indian summer monsoon. *Mon. Wea. Rev.*, **121**, 1177–1194, doi:[10.1175/1520-0493\(1993\)121<1177:STEOMF>2.0.CO;2](https://doi.org/10.1175/1520-0493(1993)121<1177:STEOMF>2.0.CO;2).
- Sperber, K., H. Annamalai, I. Kang, A. Kitoh, A. Moise, A. Turner, B. Wang, and T. Zhou, 2013: The Asian summer monsoon: An intercomparison of CMIP5 and CMIP3 simulations on the late 20th century. *Climate Dyn.*, **41**, 2711–2744, doi:[10.1007/s00382-012-1607-6](https://doi.org/10.1007/s00382-012-1607-6).
- Stephens, G., P. Webster, R. Johnson, R. Engelen, and T. L'Ecuyer, 2004: Observational evidence for the mutual regulation of the tropical hydrological cycle and tropical sea surface temperatures. *J. Climate*, **17**, 2213–2224, doi:[10.1175/1520-0442\(2004\)017<2213:OEFTMR>2.0.CO;2](https://doi.org/10.1175/1520-0442(2004)017<2213:OEFTMR>2.0.CO;2).
- Stern, W., and K. Miyakoda, 1995: Feasibility of seasonal forecasts inferred from multiple GCM simulations. *J. Climate*, **8**, 1071–1085, doi:[10.1175/1520-0442\(1995\)008<1071:FOSFIF>2.0.CO;2](https://doi.org/10.1175/1520-0442(1995)008<1071:FOSFIF>2.0.CO;2).
- Taniguchi, K., and T. Koike, 2006: Comparison of definitions of Indian summer monsoon onset: Better representation of rapid transitions of atmospheric conditions. *Geophys. Res. Lett.*, **33**, L02709, doi:[10.1029/2005GL024526](https://doi.org/10.1029/2005GL024526).
- Timmermann, R., H. Goosse, G. Madec, T. Fichefet, C. Etheb, and V. Duliére, 2005: On the representation of high latitude processes in the ORCA-LIM global coupled sea ice ocean model. *Ocean Modell.*, **8**, 175–201, doi:[10.1016/j.ocemod.2003.12.009](https://doi.org/10.1016/j.ocemod.2003.12.009).
- Uppala, S., and Coauthors, 2005: The ERA-40 re-analysis. *Quart. J. Roy. Meteor. Soc.*, **131**, 2961–3012, doi:[10.1256/qj.04.176](https://doi.org/10.1256/qj.04.176).
- Valcke, S., L. Terray, and A. Piacentini, 2000: The OASIS coupler user guide version 2.4. Tech. Rep. TR/CMGC/00-10, CERFACS, 85 pp.
- Vichi, M., E. Manzini, P. Fogli, A. Alessandri, L. Patara, E. Scoccimarro, S. Masina, and A. Navarra, 2011: Global and regional ocean carbon uptake and climate change: Sensitivity to an aggressive mitigation scenario. *Climate Dyn.*, **37**, 1929–1947, doi:[10.1007/s00382-011-1079-0](https://doi.org/10.1007/s00382-011-1079-0).
- Vitart, F., and F. Molteni, 2009: Dynamical extended range prediction of early monsoon rainfall over India. *Mon. Wea. Rev.*, **137**, 1480–1492, doi:[10.1175/2008MWR2761.1](https://doi.org/10.1175/2008MWR2761.1).
- Wang, B., and Z. Fan, 1999: Choice of South Asian summer monsoon indices. *Bull. Amer. Meteor. Soc.*, **80**, 629–638, doi:[10.1175/1520-0477\(1999\)080<0629:COSASM>2.0.CO;2](https://doi.org/10.1175/1520-0477(1999)080<0629:COSASM>2.0.CO;2).
- , I. Kang, and J.-Y. Lee, 2004: Ensemble simulations of Asian–Australian monsoon variability by 11 AGCMs. *J. Climate*, **17**, 803–818, doi:[10.1175/1520-0442\(2004\)017<0803:ESOAMV>2.0.CO;2](https://doi.org/10.1175/1520-0442(2004)017<0803:ESOAMV>2.0.CO;2).
- , Q. Ding, X. Fu, I. Kang, K. Jin, J. Shukla, and F. Doblas-Reyes, 2005: Fundamental challenge in simulation and prediction of summer monsoon rainfall. *Geophys. Res. Lett.*, **32**, L15711, doi:[10.1029/2005GL022734](https://doi.org/10.1029/2005GL022734).
- , —, and P. Joseph, 2009: Objective definition of the Indian summer monsoon onset. *J. Climate*, **22**, 3303–3316, doi:[10.1175/2008JCLI2675.1](https://doi.org/10.1175/2008JCLI2675.1).
- Webster, P., 2013: Improve weather forecasts for the developing world. *Nature*, **493**, 17–19, doi:[10.1038/493017a](https://doi.org/10.1038/493017a).
- , and C. Hoyos, 2004: Prediction of monsoon rainfall and river discharge on 15–30-day time scales. *Bull. Amer. Meteor. Soc.*, **85**, 1745–1765, doi:[10.1175/BAMS-85-11-1745](https://doi.org/10.1175/BAMS-85-11-1745).
- , V. Magana, T. Palmer, J. Shukla, R. Tomas, M. Yanai, and T. Yasunari, 1998: Monsoons: Processes, predictability and the prospects for prediction. *J. Geophys. Res.*, **103**, 14 451–14 510, doi:[10.1029/97JC02719](https://doi.org/10.1029/97JC02719).
- Weisheimer, A., and Coauthors, 2009: ENSEMBLES: A new multi-model ensemble for seasonal-to-annual predictions—Skill and progress beyond DEMETER in forecasting tropical Pacific SSTs. *Geophys. Res. Lett.*, **36**, L21711, doi:[10.1029/2009GL040896](https://doi.org/10.1029/2009GL040896).
- Wilks, D., 2006: *Statistical Methods in the Atmospheric Sciences*. 2nd ed. Academic Press, 630 pp.
- World Meteorological Organization, 2010: Manual on the Global Data-Processing and Forecasting System. Attachment II, Global Aspects, Vol. I, WMO-485, World Meteorological Organization, I.8-1–II.8-17.
- Xavier, P., C. Marzin, and B. Goswami, 2007: An objective definition of the Indian summer monsoon season and a new perspective on the ENSO-monsoon relationship. *Quart. J. Roy. Meteor. Soc.*, **133**, 749–764, doi:[10.1002/qj.45](https://doi.org/10.1002/qj.45).
- Yu, W.-D., J.-W. Shi, L. Liu, K.-P. Li, Y.-L. Liu, and H.-W. Wang, 2012: The onset of the monsoon over the Bay of Bengal: The observed common features for 2008–2011. *Atmos. Ocean Sci. Lett.*, **5**, 314–318.